

An Eight-Channel Phased Array RF Coil for Spine MR Imaging at 7 Tesla

O. Kraff^{1,2}, S. Kruszona^{1,2}, A. K. Bitz^{1,2}, S. Orzada^{1,2}, S. Maderwald^{1,2}, L. C. Schaefer^{1,2}, I. Brote^{1,2}, M. E. Ladd^{1,2}, and H. H. Quick^{1,2}

¹Erwin L. Hahn Institute for MRI, Essen, Germany, ²Department of Diagnostic and Interventional Radiology and Neuroradiology, University Hospital Essen, Essen, Germany

Introduction: With the increasing number of clinically oriented studies at 7 Tesla, radiofrequency (RF) engineers are challenged to provide new coil concepts for high-field magnetic resonance imaging (MRI) in body parts other than the head. Recent studies have shown that MRI of the spine at 3 T provides many improvements over 1.5 T spine MRI, especially in the delineation of soft tissue, cerebrospinal fluid (CSF), discs, and bone interfaces¹. Provided that the theoretical two-fold gain in signal-to-noise (SNR) from 3 T to 7 T can be clinically attained, this potentially allows improving the spatial resolution or reducing the scan time without sacrificing signal- and contrast-to-noise (CNR) ratios compared to 3 T.

Due to the improved sensitivity performance and high SNR of RF surface coils compared to volume RF coils², the phased array approach is already proven for 1.5 and 3 T imaging of the spine³. In this work we describe a transmit/receive RF array, build of eight overlapping loop coils, for imaging the human spine at 7 T. We characterize this prototype in simulations and bench measurements as well as in phantom and in vivo measurements.

Methods: The spine array was developed for a 7 T whole-body MR scanner (Magnetom 7 T, Siemens Healthcare, Erlangen, Germany) with a 60 cm bore. Eight surface loop coils with a dimension of 12 x 12 cm were machined from FR4 circuit board material (LPKF Laser & Electronics AG, Garbsen, Germany). Each coil element is 0.8 mm thick and has 1-cm-wide circuits with a copper-clad layer of 35 μ m thickness. Three 2-mm gaps were bridged by 2.7 and 4.7 pF capacitors (Voltronics Corporation, Denville, NJ, USA) on each element. Common mode cable current suppression was provided by a cable trap located directly at each coil element, formed by a 7 cm long semi-rigid coax cable wound in two turns and a variable capacitor (2.5-10 pF). Furthermore, prior finite-difference-time-domain (FDTD) simulations⁴ of the field distribution indicated use of a shifted and overlapped arrangement of the coil elements as given in Fig. 1 (left), which significantly improved the isolation between neighboring as well as to next-neighbor coils. The preamplifiers and transmit/receive (T/R) switches (Stark Contrast, Erlangen, Germany) of the coil were placed next to the spine array. Care was taken to ensure the same cable length for all eight elements, which were fed with opposite polarity between the left and right coil rows to provide a 180° phase shift. In the FDTD simulations for design optimization, a 180° phase shift increased the B_1 amplitude along the centerline of the coil, i.e. in the region of the spine, but created a signal cancellation off-center and parallel to the centerline outside the anatomy of interest. The elements were matched to 50 Ohms at 297 MHz. An image of the assembled spine array is given in Fig. 1 (right).

Tuning and matching was optimized on the bench with a phantom made of body simulating liquid ($\epsilon_r = 43$, $\sigma = 0.8 \text{ Sm}^{-1}$) and assessed with a network analyzer (Agilent E5061A). Additionally, loaded and unloaded Q values were obtained with this set-up.

A FLASH-3D sequence with TR/TE = 3.6/1.76 ms, 10° flip angle, 1 mm³ resolution, matrix 512 x 512 was used to acquire data for g-factor maps, which were calculated pixelwise by the following equation: $g\text{-factor} = \text{SNR}^{\text{full}} / (\text{SNR}^{\text{accl.}} \cdot \sqrt{R})$.

For safety validation, numerical computations⁴ of the RF field distribution and the corresponding SAR were performed based on the HUGO dataset⁴ (100 kg male) as well as on a member of the Virtual Family⁵ (70 kg male).

In vivo images of a healthy volunteer were assessed with a FLASH-3D sequence (TR/TE = 7.2/2.4, 20° flip angle, resolution 0.78 mm isotropic, matrix 512 x 512).

Results: S-parameter measurements on the bench yielded an S11 match between -15 dB and -22 dB and S12 coupling between neighboring elements in the range of -13 dB and -19 dB. The unloaded to loaded Q ratio was 1.3 for a single element in the presence of all other elements. Maximum g-factors were 1.35, 1.48, and 1.94 for GRAPPA acceleration factors R = 1.9, 2.7 and 3.5 (using 24 reference lines) in the head-foot direction, respectively.

The numerical results indicated a maximum permitted power level of 12.5 W to remain in compliance with the IEC guidelines of 10 W/kg for 10g-averaged local SAR. Comparable results were found for both calculations, i.e. with the Visual Human dataset as well as with the Virtual Family dataset.

In vivo images reveal a good excitation along the spine over a 40 cm FOV. Anatomic details such as the vertebral bodies, the dens, or the longitudinal ligaments are well visualized. In a coronal scan, the predicted B_1 signal cancellation parallel to the centerline is outside the region of interest as expected; see Fig. 3 (C).

Discussion: These early results indicate that a transmit/receive phased array can be used for in vivo spine imaging at 7 Tesla and thereby make high-resolution spine imaging a promising new application in 7 Tesla clinical research. Work is underway to assess patients with various pathologies.

References:

1. Shapiro MD. MR imaging of the spine at 3T. MRI Clinics of North America 2006;14(1):97-108.
2. Roemer PB, et al., The NMR phased array. Magn Reson Med 1990;16(2):192-225.
3. Peterson DM, et al., An MR transceive phased array designed for spinal cord imaging at 3 Tesla: preliminary investigations of spinal cord imaging at 3 T. Investigative radiology 2003;38(7):428-435.
4. CST MICROWAVE STUDIO®, CST GmbH. User Manual Version 2008. Darmstadt, Germany.
5. Virtual Family Models, http://www.itis.ethz.ch/index/index_humanmodels.html.

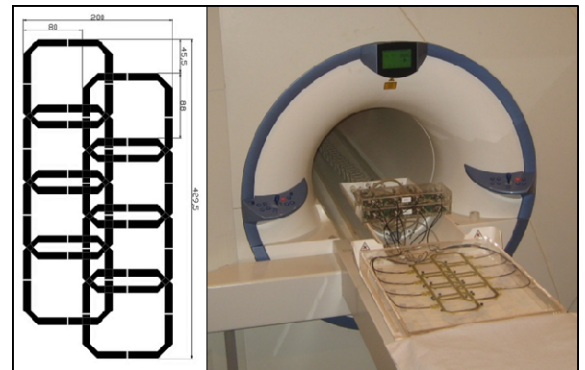


Fig. 1 – Left: Optimized arrangement of loop elements obtained from FDTD simulations. Right: Assembled spine array integrated into the patient table. T/R switches and preamplifiers are positioned behind the coil at the very end of the table.

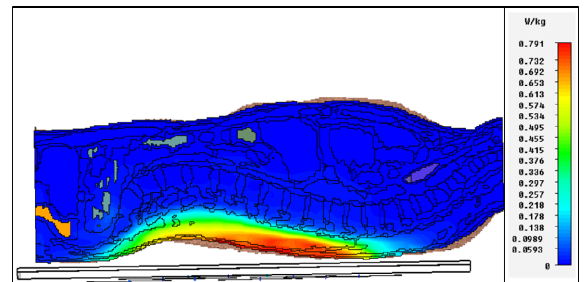


Fig. 2 – Calculation of the SAR distribution for safety validation of the spine array using the male member of the Virtual Family (10g-averaged SAR, linear scale).



Fig. 3 – In vivo FLASH-3D images of a healthy volunteer. Sagittal views of (A) cervicothoracic and (B) thoracolumbosacral spine. Note the good visualization of the dens in (A) and the anterior as well as posterior longitudinal ligament in (B). A coronal slice of the thoracic vertebrae and an enlarged coronal view of the joints and spinal cord in the cervical region are given in (C) and (D), respectively. In (E) an axial, reformatted slice through the cervical vertebrae is given.